3848–3855 *Nucleic Acids Research, 2010, Vol. 38, No. 11* *Published online 17 February 2010*
doi:10.1093/nar/gkq079

Photomodulating RNA cleavage using photolabile circular antisense oligodeoxynucleotides

XinJing Tang[1,2,*], Meng Su[1], LiLi Yu[3], Cong Lv[1], Jie Wang[2] and ZhongJin Li[3]

[1]State Key Laboratory of Natural and Biomimetic Drugs, [2]School of Pharmaceutical Sciences, Peking University No. 38, Xueyuan Rd, Beijing 100191 and [3]College of Chemistry and Chemical Engineering, Shaanxi University of Science & Technology, Xi'an 710021, Shaanxi, China

Received December 3, 2009; Revised January 26, 2010; Accepted January 27, 2010

ABSTRACT

Caged antisense oligodeoxynucleotides (asODNs) are synthesized by linking two ends of linear oligodeoxynucleotides using a photocleavable linker. Two of them (H30 and H40) have hairpin-like structures which show a large difference in thermal stability ($\Delta T_m = 17.5^\circ C$ and $11.6^\circ C$) comparing to uncaged ones. The other three (C20, C30 and C40) without stable secondary structures have the middle 20 deoxynucleotides complementary to 40-mer RNA. All caged asODNs have restricted opening which provides control over RNA/asODN interaction. RNase H assay results showed that 40-mer RNA digestion could be photo-modulated 2- to 3-fold upon light-activation with H30, H40, C30 and C40, while with C20, RNA digestion was almost not detectable; however, photo-activation triggered >20-fold increase of RNA digestion. And gel shift assays showed that it needed >0.04 μM H40 and 0.5 μM H30 to completely bind 0.02 μM 40-mer RNA, and for C40 and C30, it needed >0.2 μM and 0.5 μM for 0.02 μM 40-mer RNA binding. However, even 4 μM C20 was not able to fully bind the same concentration of 40-mer RNA. By simple adjustment of ring size of caged asODNs, we could successfully photoregulate their hybridization with mRNA and target RNA hydrolysis by RNase H with light activation.

INTRODUCTION

Manual regulation of gene expression is one of the most important scientific areas. Several technologies using oligonucleotides, such as antisense, antigene and RNA interference, have been developed. However, it is still very challenging to switch gene expression 'on' and/or 'off' and provide high spatial and temporal resolution. (1–15) Photolabile groups can be used to temporarily 'cage' oligonucleotides. Their activities can be restored by light irradiation which provides new possibilities for controlling gene expression in both space and time (2,9,16–28). Currently, there is still a strong need for more effective gene regulation tools.

For the regulation of gene expression, antisense strategies based on the hybridization of target mRNA with complementary DNA (antisense DNA) have been widely applied to gene silencing in many experimental systems and are being evaluated as treatments for cancers and other diseases in human clinical trials (29,30). Different strategies for photoregulation of gene expression have been developed. One strategy is based on application of multiple photoresponsive groups to modulate the interaction of antisense oligonucleotides (asODNs) and target RNAs. Monroe *et al.* (31) reported they could photomodulate DNA hybridization using a molecular beacon assay and determine the relative caging and uncaging percentages for 20-mer oligodeoxynucleotide with an average 14–16 nitrophenyl caging groups. While Komiyama *et al.* (32) incorporated azobenzene groups into the sense strand and controlled the hybridization of sense strand and antisense strand to regulate target RNA digestion through azobenzene photoisomerization. However, multiple azobenzene groups are a must for reasonable photomodulation. Recently, Deiters *et al.* (33) applied a new photocleavable nitrobenzyl derivative for caging thymidine at N′ position to disturb the A–T hydrogen binding. They could photoregulate luciferase expression in cells with 3 or 4 caging thymidines for 18-mer asODNs. For multiple photolabile groups, complete uncaging requires much high intensity UV light and long-time irradiation. Another strategy is focused on single photolabile linker for photomodulation. There were some reports about the mechanism of light-triggered strand break of oligonucleotides (34–36). For gene-related studies of interaction of asODN with DNA or RNA, pioneering work done by Taylor *et al.* (37) demonstrated the incorporation

*To whom correspondence should be addressed. Tel/Fax: +86 10 82805635. Email: xinjingt@bjmu.edu.cn

of a photoactive *o*-nitrobenzyl moiety bridging within the phosphate backbone of a DNA hairpin and the application to trigger DNA/DNA duplex formation. Near UV irradiation under ambient conditions triggered a strand break which released 18-mer oligodeoxynucleotide to bind a complementary DNA strand with a 9-fold greater affinity. More recent examples were presented by Dmochowski *et al.* (38–40) using a short complementary sense strand as the blocking moiety for an asODN with a heterobifunctional photocleavable linker. In these examples, multiple basepairs worked as multiple caging groups and the relative thermostability of asODN-PL-sODN and asODN/sODN duplex was used to control the asODN/RNA hybridization and RNA digestion in RNase H assay, and in cells and zebrafish. Based on this simple design, Friedman (41) and Chen (42,43) further respectively extended their applications in RNA interference in cells and morpholino oligonucleotides for targeting gene expression in zebrafish. However, this design was dependent on the relative thermostability of asODN-PL-sODN, asODN/sODN and asODN/RNA, which would be greatly effected in complicated cellar environments. Sometimes the best candidate in *in vitro* selection was not the best one in cells (40). More general and effective light-activated asODNs are still needed.

Based on many biological processes that involve the hybridization of DNA/DNA, DNA/RNA or RNA/RNA, we have sought to develop chemically synthetically facile and high-quantum efficient routes for photomodulating the hybridization of asODNs to target DNA or mRNA molecules (38). Most recently Dmochowski *et al.* (44) reported a photocleavable circular DNAzyme through enzymatic coupling of two ends of oligodeoxynucleotide for controlling RNA digestion. Here, we developed a general strategy of linking two ends of a linear asODNs using a photocleavable linker. These caged circular asODNs were restricted from extending to bind their targets and their activities were masked until light cleaved the linker and released two ends of asODNs. Previously, similar strategies used in photoregulation of asODN/RNA were based on relative thermostability of caged asODN, asODN/sODN and asODN/RNA. In this study, we aim to photomodulate asODN/RNA hybridization sterically and thermodynamically, as shown in Scheme 1.

Here, we reported a new design of caged asODNs. End-linked circular photolabile asODNs with 1-(2-nitrophenyl)-1,2-ethanediol (**PL**) photolabile moiety incorporated in the asODN sequences were designed to regulate hybridization of asDNAs and target RNA and/or photomodulate RNA digestion by RNase H. A linear asODN is usually flexible and has random structure, however when it hybridizes with a complementary RNA, the duplex will become much rigid and extended. Within a limited length of deoxynucleotides in an oligodeoxynucleotide ring, the formation of duplex will be efficiently inhibited. Five different length end-linked caged asODNs are synthesized and used in this work. Two of the circular caged asODNs (**H30** and **H40**) have the hairpin-like structure. One is a 30-mer end-linked caged asODN

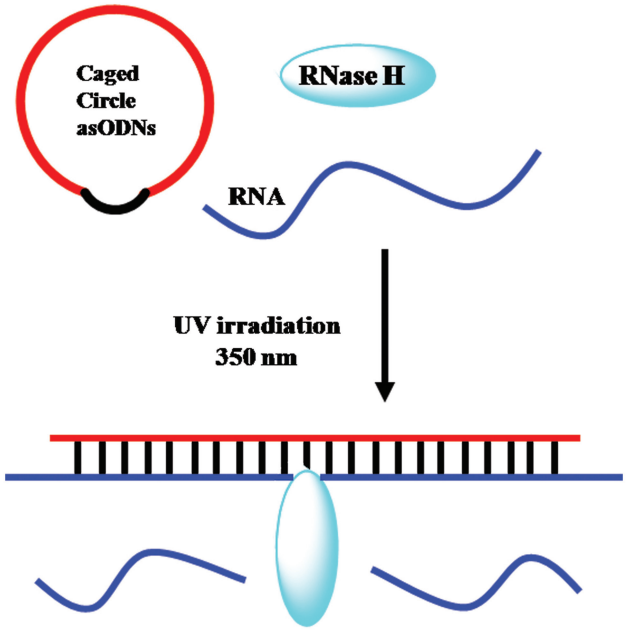

Scheme 1. Strategy for photoregulating RNA digestion using caged circular asODNs.

(**H30**) with a 5-deoxynucleotide-paired stem and a 20-deoxynucleotide hairpin loop, the other one (**H40**) is a 40-mer end-linked asODN hairpin (**H40**) with another five non-complementary deoxynucleotides at both ends of **H30**. The other three caged asODNs (**C20**, **C30** and **C40**) without stable secondary structures have different numbers of deoxynucleotides in the ring, but share the same 20-deoxynucleotide sequence in the middle. Caged asODNs, **C20**, **H30** and **H40**, have 20, 30 and 40 paired bases with the 40-mer RNA target respectively, while **C30** and **C40** have the same middle 20 deoxynucleotides as **C20** which are base-paired with the middle 20 nucleotides of the 40-mer RNA (Scheme 2). All these end-linked caged circular asODNs have restricted opening of oligodeoxynucleotide rings, which provides control over RNA/asODN duplex formation and targets RNA digestion by RNase H.

MATERIALS AND METHODS

General methods

All single-stranded oligodeoxynucleotides were custom-synthesized with C7 amino modified CPG and purified with an Agilent 1200 HPLC system using a reverse-phase analytical HPLC column (reverse phase C18, 4.6×250 mm, 5 μm beads). The concentrations of all oligodeoxynucleotides were measured in water at 260 nm using a Varian Cary 300 UV/Vis spectrophotometer. Melting studies were carried out with a Varian Cary 300 UV/Vis spectrophotometer. Gels of RNA digestion were imaged using an Amersham Biosciences Storm 840 phosphorimager and quantified with ImageQuant software (ImageQuant^{TM} TL v2005, GE Healthcare). All photoirradiation experiments with

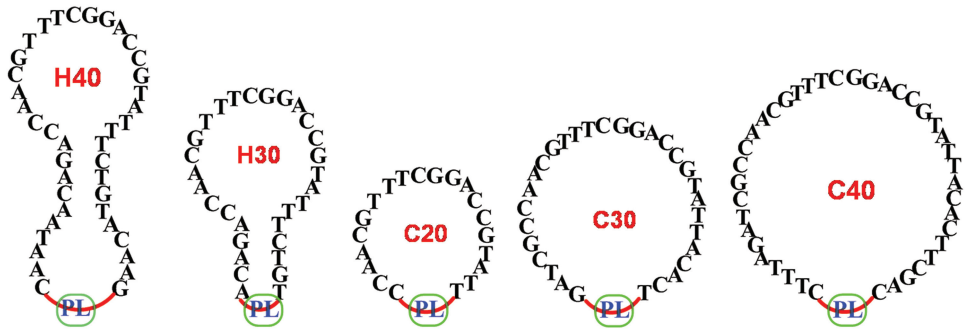

Scheme 2. Sequences and structures of caged circular asODNs. **H30** and **H40** with hairpin-like structure are fully complementary to a 40-mer RNA. **C20**, **C30** and **C40** share the same 20-mer nucleotide sequence in the middle which is complementary to the middle 20 nucleotides of the 40-mer target RNA.

oligodeoxynucleotide samples were carried out with a xenon lamp (450 W) and monochromator (20 nm slit centered at 350 nm, 30 mW/cm^2 at the sample). Standard 1× RNase H reaction buffer was defined as 20 mM Tris–HCl, 20 mM KCl, 10 mM $MgCl_2$, 0.1 mM EDTA, and 0.1 mM DTT, pH 8.0. The melting temperature measurements used the same RNase H buffer.

Synthesis of photolabile circular asODNs

CPG with 3′-end amino modification was used for oligodeoxynucleotide synthesis. All oligodeoxynucleotide sequences for **H30**, **H40**, **C20**, **C30** and **C40** were custom-synthesized according to the standard DNA synthesis. At the 5′-end of the sequences was attached with 1-(2-nitrophenyl)-1,2-ethanediol (**PL**) phosphoroamidite (see Supplementary Material for synthesis), following by the amino group (MMT protected) with C6 attached to sequences through phosphorodiester bonds. MMT was then removed by 4%TFA in CH_2Cl_2 to release 5′ amino group. Before cleavage from the resin, the amino group first reacted with about 100 fold excess succinic anhydride and N,N-diisopropylethylamine (DIPEA) in 0.5 ml DMF at room temperature overnight.

Sequences used in the study:

C20-COOH: 5′-$HOOCCH_2CH_2CONHC_6$-PL-CCAACG TTTCGGACCGTATT–C_7-NH_2

H30-COOH:5′-$HOOCCH_2CH_2CONHC_6$-PL-ACAGAC CAACGTTTCGGACCGTATTTCTGT–C_7NH_2

H40-COOH: 5′-$HOOCCH_2CH_2CONHC_6$-PL-CAATAA CAGACCAACGTTTCGGACCGTATTTCTGTACA AG–C_7NH_2

C30-COOH: 5′-$HOOCCH_2CH_2CONHC_6$-PL-GATCGC CAACGTTTCGGACCGTATTACACT–C_7NH_2

C40-COOH: 5′-$HOOCCH_2CH_2CONHC_6$-PL–CTTTAG ATCGCCAACGTTTCGGACCGTATTACACTTCG AC–C_7NH_2

The oligodeoxynucleotides were then cleaved from resin and deprotected using concentrated ammonium hydroxide. After removal of ammonia, the oligodeoxynucleotides were purified with HPLC under reverse phase conditions: A, 0.05 M TEAA; B, acetonitrile; B, 0–15% in 30 min, 15–45% in 30 min. The product peak was collected and characterized by ESI-MS using negative mode (1% TEA in H_2O/CH_3CN). **C20**-COOH, calculated: 6801.0; measured: 6800.0; **H30**-COOH, calculated: 9890.3, measured: 9890.45; **H40**-COOH, calculated: 12981.3, measured: 12981.15; **C30**-COOH, calculated: 9875.0; measured: 9875.0; **C40**H-COOH, calculated: 12914.9; measured: 12915.6.

The oligodeoxynucleotides with amine and acid groups at two terminal ends were dried and ethanol-precipitated with 3 M NaCl to remove the TEAA residue. Twenty nanomoles precipitated oligodeoxynucleotides were dissolved in 2 ml 0.1 M MES buffer (pH = 6.5), 0.3 M NaCl and 10 mM $MgCl_2$ with final concentration of 5 mM HOBt. Then ~1 mg 1-ethyl-3-(3-dimethylaminopropyl) carbodiimide, hydrochloride (EDAC) was added into the oligodeoxynucleotide solutions. The mixture was vortexed and stood at room temperature for 10–14 h.

The solutions were then desalted using NAP-10 columns, following by RP HPLC purification (A, 0.05 M TEAA; B, acetonitrile; B, 0–15% in 30 min, 15–45% in 30 min, running temperature, 40°C). The retention time of product peaks were usually 1–2 min longer than those of starting oligodeoxynucleotides. The collected products were subject to dry in vacuum and characterized by ESI-MS. The yields were calculated by dissolved the caged circular oligodeoxynucleotides in water and measured the absorbance at 260 nm. The synthetic yields for caged circular oligodeoxynucleotides were 20–40% under our synthetic conditions. ESI-MS was carried out under negative mode (1% TEA in H_2O/CH_3CN). **C20**, calculated: 6782.0; measured: 6782.0; **H30**, calculated: 9872.3, measured: 9871.55 + n Na^+; **H40**, calculated: 12 963.3, measured: 12 961.25 + n Na^+, measured: **C30**, calculated: 9857; measured: 9854.8; **C40**, calculated: 12897.6; measured: 12 895.7.

Thermal denaturation studies

Thermal denaturation studies were performed on **H30**, **H40**, their uncaged **H30, H40**, uncaged **H30, H40** with

target RNA in standard RNase H buffer. The concentration of each asODN was determined by dissolving it in pure water and measuring the absorbance at 260 nm. The solution was heated to 90°C for 5 min, and allowed to cool gradually to 20°C. Samples were monitored at 260 nm while heating or cooling at a rate of 0.5°C/min. Melting temperatures were determined from the peak of the first derivative plot of Abs_{260} versus temperature.

RNase H assays

The 40-mer RNA target sequence (5′-CUUGUACAGAA AUACGGUCCGAAACGUUGGUCUGUUAUUG-3′) in HPLC-pure form, was purchased from Shanghai GenePharma Co, Ltd. Recombinant RNase H from *E. coli* and the reaction buffer were purchased from Epicentre Biotechnologies. The standard procedure for the RNase H assay was as follows: a caged circular asODN was incubated in 1× ribonuclease H reaction buffer at 37°C, [γ-^{32}P]-labeled RNA oligonucleotide (200-fold excess) was added and incubated at 37°C for 20 min to allow RNA/DNA duplex formation. RNase H (2 U) was then added to the mixture and incubated at 37°C. Total reaction volume was 20 μl, and the final concentrations of asODNs and RNA were 0.02 μM and 4 μM, respectively.

To measure RNA degradation by RNase H after photoactivation, the DNA conjugates were UV-illuminated by Xe lamp through monochromator (350 nm UV light generated by 450 W Xenon lamp after passing through monochromator, ~30 mW/cm^2), [γ-^{32}P]-labeled RNA oligonucleotide was added and incubated at 37°C for 20 min to allow RNA/DNA duplex formation. RNase H assays were performed as described above. Time points were taken at 2, 5, 10, 15 and 30 min by sampling 4 μl of the reaction mixture, adding 6 μl gel loading buffer (50 mM EDTA, 90% formamide with bromphenol blue and xylene cyanol, total volume = 10 μl), and then heating the solutions to 95°C for 3 min to terminate the reaction.

All of the resulting solutions were subject to electrophoresis on a 20% polyacrylamide gel containing 7 M urea. Intensity values of gel bands were integrated in ImageQuant for each band with automated lane and band finding using a local method background correction in the gel lane. The relative amount of RNA digestion was determined by dividing the intensity of the band corresponding to cleaved RNA by the total intensity of the cleaved and uncleaved RNA bands.

Gel shift assays

To determine the binding of RNA to the caged circular asDNAs, gel mobility shift assays were performed as described in the literature (45). [γ-^{32}P]-labeled 40-mer RNA was used in this study, and the binding of a fixed concentration of the 40-mer RNA (0.02 μM) with increased concentrations of caged circular asODNs was carried out in 9 μl RNase H buffer containing 20 mM Tris–HCl, 20 mM KCl, 10 mM $MgCl_2$, 0.1 mM EDTA, 0.1 mM DTT, pH 8.0. Samples were annealed at 37°C for 30 min and then were put into ice water. Before the samples were loaded into the gel, 1 μl glycerol with bromphenol blue and xylene cyanol was added. All 10 μl solutions were loaded into 12% native polyacrylamide gels. The gels were then electrophoresed at 100 V for 2 h at 10°C, using 1 × TBE buffer (pH = 8.2). Gels were exposed and then imaged with a Storm phosphorimager.

RESULTS AND DISCUSSION

Design and optimization of photolabile circular asODNs

The hybridization between an asODN and a sense RNA is one of the key factors in RNA digestion by RNase H. Previous works on related research with a single photolabile group in asODNs are based on the relative thermostability of three components in the system (caged asODN, asODN/sODN and asODN/RNA); however, it takes quite efforts to adjust the system to find the right pair. Steric inhibition of asODN/RNA is another way to achieve the same results. However, a single caging group attached to a 20-mer asODN is not enough to compensate the large thermodynamic driving force and have proven relatively ineffective (31,46,47).

Based on the natural properties of the oligodeoxynucleotide, a linear asODN is usually flexible and has random conformations. However, once it hybridizes with a complementary DNA or RNA strand, the duplex will become much rigid and extended. Within a limited length of deoxynucleotides in an oligodeoxynucleotide ring, formation of the duplex will be efficiently inhibited, and once the caged circular asODN is released by the light, it will quickly interact with its target RNA. Two different length end-linked caged asODNs (**H30** and **H40**) are first synthesized. One is a 30-mer end-linked asODN (**H30**) with a 5 nucleobase-paired stem and a hairpin loop with 20 deoxynucleotides, the other one is a 40-mer end-linked caged asODN (**H40**) with another 5 non-complementary deoxynucleotides at both ends of **H30**. A 40-mer RNA that is complementary to **H30** and **H40** is used to hybridize with the asODNs and further evaluate the photomodulation of its digestion by RNase H. Another three end-linked caged circular asODNs (**C20**, **C30** and **C40**) do not have stable secondary structures, and the middle 20 nt of **C30** and **C40** share the same sequence with **C20** which is complementary to the middle 20 nucleotide sequence of the target 40-mer RNA. All these three caged asODNs are used to study their interaction with the target 40-mer RNA.

We measured the melting temperatures of uncaged asODNs (**H30** and **H40**), caged asODNs (**H30** and **H40**) and duplexes of uncaged asODNs (**H30** and **H40**) with the 40-mer target RNA. The melting temperatures of uncaged **H30** and **H40** were both ~ 42°C under the same buffer conditions as RNase H assay, because these two oligodeoxynucleotides had exactly the same loop size and stem bases except that **H40** had 5 extra non-complementary deoxynucleotides on each end. However for the end-linked caged **H30** and **H40**, the melting temperatures were 59.5°C and 53.6°C, respectively, which were 17.5°C and 11.6°C higher than uncaged **H30** and **H40**. And the caged **H30** was more

stable than the caged **H40** due to the extra 10-base loop for **H40** which destabilized the hairpin. We also measured the T_m of duplexes of uncaged **H30** and **H40** with the 40-mer target RNA, which were 77.3°C and 79.3°C, respectively.

Photomodulation of RNA digestion by RNase H with caged circular asODNs

RNA cannot be digested by RNase H without the existence of complementary antisense strand. Under current RNase H assay conditions with 4 μM [γ-^{32}P]-labeled target 40-mer RNA, 0.02 μM asODN, and 2 U RNase H in standard RNase H buffer at 37°C, there was almost no RNA digestion detectable with caged asODN **C20** up to 30 min incubation time before UV irradiation. However, UV irradiation (350 nm UV light generated by 450 W Xenon lamp after passing through monochromator, ~30 mW/cm^2) triggered the chemical bond cleavage and promoted interaction between uncaged **C20** and target RNA. Figure 1 showed a typical gel that the cleaved RNA at the lower band gradually increased, and RNA digestion reached up to 27.5% in 30 min, which was at least >20-fold increase in comparison to **C20** in the dark. While with the fully complementary caged circular **H30** and **H40**, about 79% target RNA was digested in 30 min after UV irradiation, which was about 3- and 2-fold increase of 40-mer target RNA digestion compared to **H30** and **H40** before light-activation, respectively. The results showed that RNA digestion did not increase after UV photoactivation even though **H40** had 10 more paired bases than **H30**. However, 'background' RNA cleavage for **H40** in the dark was much higher than **H30** and **C20**. Clearly, **H40** was fully complementary to the 40-mer target sequence, so the binding energy of the duplex was much larger than that of **H30** or **C20**. **H40** also had larger circle than **H30** or **C20**, and it was much easier for 40-mer RNA to wind around **H40** than **H30** or **C20**, which should be less efficient to photomodulate target RNA digestion by RNase H.

To confirm which is the most important factor for photomodulation of RNA digestion between ring size and the number of paired bases, another two caged circular asODNs (**C30** and **C40**) were introduced with 30 and 40 deoxynucleotides as **H30** and **H40,** respectively, but only had the middle 20 deoxynucleotides complementary to the middle 20 nucleotide sequence of the 40-mer RNA target. Under the same RNase H assay conditions, around 50% 40-mer RNA was digested by RNase H in 30 min for both light-activated **C30** and **C40** which were 2- and 1.9-fold more than caged circular asODNs, **C30** and **C40** as shown in Figure 2. Comparing **C30** with **H30**, **C40** with **H40**, RNase H assay results showed that there was RNA digestion increase by RNase H (from 25%, 26% for **C30** and **C40** to 28%, 40% for **H30** and **H40**) in the 'caged' state of circular asODNs, which was due to the more paired nucleotides and binding energy between asODNs and the 40-mer target RNA. In comparison with **C20**, **C30** and **C40** in the caged state, **C20** with smaller 20-deoxynucleotide ring almost had no detectable 40-mer target RNA digestion, while there were 25% and 26% of target RNA cleaved for **C30** and **C40** by RNase H under the same conditions. And the photomodulation efficiency for **C30** and **C40** is much smaller than **C20,** which is at least >20-fold increase of RNA digestion with light activation when the ring was as small as a 20-mer oligodeoxynucleotide. To further prove that the ring size did matter for photoregulation of a certain length of RNA digestion by RNase H, we replaced the 40-mer target RNA with a shorter 20-mer RNA (5′-*AAUACGGUCCG AAACGUUGG*-3′) that was complementary to the

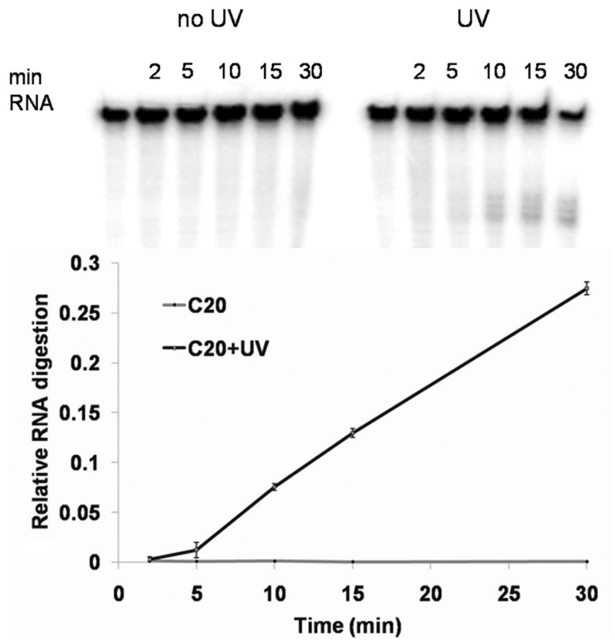

Figure 1. Denaturing PAGE (20%) analysis of RNA digestion with 4 μM [γ-^{32}P]-labeled 40-mer target RNA, 0.02 μM caged circular asODN (**C20**) and 2 U RNase H in 20 μl RNase H buffer at 37°C. Uncaged **C20** had been irradiated with UV light (350 nm, ~30 mW/cm^2) for 10 min. The charts were the cleavage percentage of the 40-mer RNA by RNase H at different time points quantified with ImageQuant. Each point is the average of two or three separate trials.

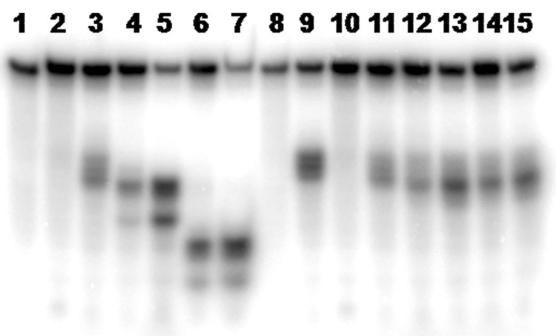

Figure 2. Denaturing PAGE (20%) analysis of RNA digestion in 30 min with 4 μM [γ-^{32}P]-labeled 40-mer RNA, 0.02 μM caged asODNs in 20 μl RNase H buffer with 2 U RNase H at 37°C. Lanes 1, RNA marker; lane 2, **C20**; lane 3, **C20** + UV; lane 4, **H30**; lane 5, **H30** + UV; lane 6, **H40**; lane 7, **H40** + UV; lane 8, RNA marker; lane 9, linear control asODN (20-mer); lane 10, **C20**; lane 11, **C20** + UV; lane 12, **C30**; lane 13, **C30** + UV; lane 14, **C40**; lane 15, **C40** + UV. Samples were photocleaved with UV light (350 nm, ~30 mW/cm^2) for 10 min.

sequence of **C20**. RNase H assay results with the 20-mer RNA showed that the 20-mer RNA was readily digested by RNase H even though **C20** was in the 'caged' state (see Supplementary Figure S5). The result was not surprising, as we knew the short RNA would wind around the caged circular **C20** more easily than the longer RNA due to the requirement of the helix structure for duplex formation. So the relative size of a cagd asODN ring and its target RNA was the most important factor to photomodulate the RNA digestion. For **C20**, it could not be used to photoregulate the 20-mer RNA digestion by RNase H. However, it was able to efficiently photocontrol a 40-mer target RNA digestion. For the large ring size of asODNs as **H30**, **H40**, **C30** and **C40**, we expect they might readily photoregulate longer RNA digestion, such as mRNA in cells.

Binding of RNA with caged circular asODNs

RNA cleavage by RNase H is a three-component system requiring the presence of a target RNA, an asODN and RNase H. RNase H binds to the RNA/asODN duplex, and then the RNA cleavage event can happen. To examine our design strategy, gel shift assays of interaction between the RNA and caged circular asODNs were used. We fixed the concentration of the 40-mer RNA at 0.02 μM in 10 μl RNase H buffer, then different ratios of asODN/RNA were used to determine the relative binding ability of the 40-mer RNA to caged circular asODNs. Unsurprisingly, the native gel assays indicated that only 0.04 μM of **H40** was able to bind all of the RNA and form duplex, while it needed >0.5 μM **H30** to form the duplex with the same amount of the RNA (see Supplementary Data). For caged circular asODNs such as **C30** and **C40**, the native gel assays indicated that 0.2 μM **C40** were needed for binding most of the 40-mer RNA and forming the stable duplex. Compared to **H40**, **C40** had less complementary deoxynucleotides, which needed more caged asODN in order to fully occupy the 40-mer RNA. However, it needed more than 0.5 μM caged asODNs for both C**30** and **H30** to bind the same amount of the 40-mer RNA, which showed that the ring size of caged asODNs was the decision-maker for RNA binding. Gel shift assay result of **C20** further confirmed that the ring size was the most important to binding affinity of the caged circular asODNs with the target RNA. For the 40-mer RNA, even 4 μM of **C20** could not fully bind all of the RNA, and bound much less efficiently than **C30** and **C40**, as shown in Figure 3. These results were consistent with RNase H assay experiments.

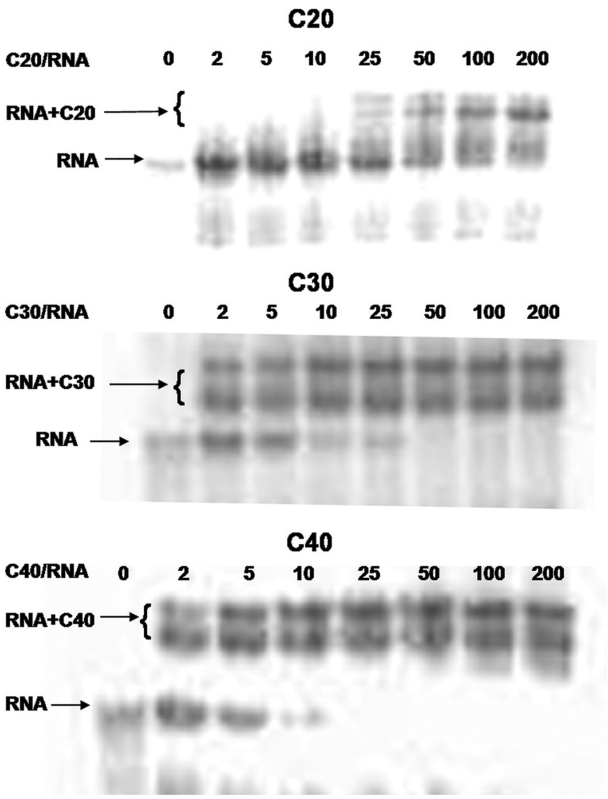

Figure 3. Native PAGE gels of binding of the 40-mer RNA with different concentrations of **C20, C30** and **C40**. The solutions of the 40-mer RNA (0.02 μM) with different concentration ratios of **C20**, **C30** or **C40** (from 1: 2 to 1: 200) in 10 μl RNase H buffer was used for binding assays. The mixtures were first mixed in 9 μl RNase H buffer and then incubated at 37°C for 30 min. After that, the solution was put inside ice water and added around 1 μl glycerol with bromphenol blue and xylene cyanol. Then the mixtures were loaded into a 12% native gel and the gel was run under 100 V at 10°C.

RNA cleavage profile of caged circular asODNs

Interestingly, the position of RNA cleavage by RNase H was different for caged **H40** from other caged circular asODNs, even though the antisense sequence of **H30** covered the middle 30 deoxynucleotides of **H40**. The RNase H cleavage site was mapped using a 5′-end-P^{32} radiolabeled RNA probe. An alkaline RNA ladder was included to identify each nucleotide and enable sequence identification. The main cutting point was the phosphodiester bond of A and C for **H30**, and the phosphodiester bond of A and G for **H40**, as shown in Figure 4. To confirm that the short fragment of RNA with the **H40** existence was not the second cleavage by

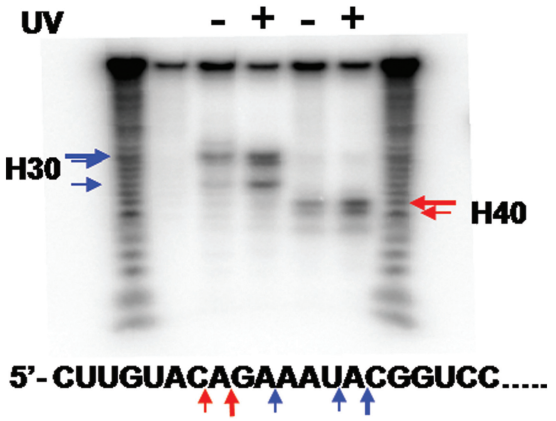

Figure 4. Mapping of the 40-mer RNA cleavage by RNase H with the presence of **H30** and **H40** with and without UV irradiation. Essays were done in 30 min with 25U RNase H, 4 μM RNA and 0.02 μM **H30** or **H40** in 20 μl RNase H buffer at 37°C. A RNA ladder was prepared from the 40-mer RNA using sodium carbonate at 90°C. Arrows showed the cleavage position and thickness of arrows represented major or minor cleavage.

RNase H, time dependent of RNA digestion was studied. From time point 2–30 min, the cleavage profile was the exact same without any intermediate cleavage fragment (See Supplementary Data). The results showed that RNase H could prefer binding the certain sequences and cutting the specific RNA phosphodiester bonds. The caged asODN and linear asODN had the same RNA cleavage patterns, and UV activation did not change the cleavage position of the RNA.

CONCLUSION

We designed a new type of caged asODNs with a single photolabile linker and end-linked circular structure. Two of the circular caged asODNs (**H30** and **H40**) have the hairpin-like structures which are much more stable than their related uncaged antisesne ODNs with melting temperature increase as high as 17.5°C and 11.6°C, respectively. The other three caged circular asODNs (**C20**, **C30** and **C40**) with different numbers of deoxynucleotides in the ring do not have stable secondary structures. All these caged circular asODNs have restricted opening of oligodeoxynucleotide rings, which provides control over RNA/asODN duplex formation. RNase H assay results showed that the 40-mer RNA digest was photomodulated about 2- to 3-fold upon light activation with caged **H30**, **H40**, **C30** and **C40**, while with the presence of caged circular **C20**, RNA digestion was almost not detectable before light activation, however, photoactivation triggered >20-fold increase of RNA digestion by RNase H. And gel shift assays showed that it needed >0.04 μM and 0.5 μM of **H40** and **H30** in 10 μl solution to completely bind a fixed concentration (0.02 μM) of the 40-mer RNA. For caged **C40** and **C30**, it needed >0.2 μM and 0.5 μM caged asODNs to fully bind the fixed concentration of the 40-mer RNA. However, even 4 μM of **C20** was not able to completely bind the fixed concentration of the 40-mer RNA. But the replacement of the 40-mer RNA with a 20-mer RNA caused RNA to efficiently interact with caged **C20**, and assay results showed that the 20-mer RNA easily bound caged **C20** and was readily digested by RNase H even without light activation. By simply adjusting the ring size of caged circular asODNs, we succeeded in photomodulating the 40-mer RNA hybridization and digestion by RNase H. Based on the results of **C20**, **C30**, **C40**, **H30** and **H40**, the ability of their interaction to target RNA showed that using smaller loop of caged circular asODNs or longer RNA helped increase the photomodulation efficiency of RNA digestion by RNase H. We expect that these types of photolabile circular asODNs can be quickly released upon light activation. And the uncaged asODNs can subsequently interact with the target RNA, successfully regulate their hybridization with mRNA, and target RNA hydrolysis by RNase H. More studies of optimization of caged end-linked circular asODNs and their *in vivo* applications are on the way. And RNA degradation profile also showed that RNA digestion with the presence of caged circular asODNs did not change the RNA cleavage pattern by RNase H before and after light activation.

SUPPLEMENTARY DATA

Supplementary Data are available at NAR Online.

ACKNOWLEDGEMENTS

We thank State Key Laboratory facility for instrumental support and technical assistance.

FUNDING

Start-up fund came from State Key Laboratory of Natural and Biomimetic Drugs (Key Laboratory Grant) and Peking University "985" foundation (bmu-2009137-121). Funding for open access charge: Start-up fund.

Conflict of interest statement. None declared.

REFERENCES

1. Shi,Y. and Koh,J.T. (2004) Light-activated transcription and repression by using photocaged SERMs. *ChemBioChem.*, **5**, 788–796.
2. Shah,S., Rangarajan,S. and Friedman,S.H. (2005) Light-activated RNA interference. Angew. *Chem., Int. Ed. Engl.*, **44**, 1328–1332.
3. Shoham,S., O'Connor,D.H., Sarkisov,D.V. and Wang,S.S.-H. (2005) Rapid neurotransmitter uncaging in spatially defined patterns. *Nat. Meth.*, **2**, 837–843.
4. Rothman,D.M., Petersson,E.J., Vazquez,M.E., Brandt,G.S., Dougherty,D.A. and Imperiali,B. (2005) Caged phosphoproteins. *J. Am. Chem. Soc.*, **127**, 846–847.
5. Pollitt,S.K. and Schultz,P.G. (1998) A photochemical switch for controlling protein-protein interactions. *Angew. Chem., Int. Ed. Engl.*, **37**, 2104–2107.
6. Wu,N., Deiters,A., Cropp,T.A., King,D. and Schultz,P.G. (2004) A genetically encoded photocaged amino acid. *J. Am. Chem. Soc.*, **126**, 14306–14307.
7. Lima,S.Q. and Miesenbock,G. (2005) Remote control of behavior through genetically targed photostimulation of neurons. *Cell*, **121**, 141–152.
8. Adesnik,H., Nicoll,R.A. and England,P.M. (2005) Photoinactivation of native AMPA receptors reveals their real-time trafficking. *Neuron*, **48**, 977–985.
9. Ando,H., Furuta,T., Tsien,R.Y. and Okamoto,H. (2001) Photo-mediated gene activation using caged RNA/DNA in zebrafish embryos. *Nat. Genet.*, **28**, 317–325.
10. Ando,H., Furuta,T. and Okamoto,H. (2004) Photo-mediated gene activation by using caged mRNA in zebrafish embryos. *Meth. Cell Biol.*, **77**, 159–171.
11. Banghart,M., Borges,K., Isacoff,E., Trauner,D. and Kramer,R.H. (2004) Light-activated ion channels for remote control of neuronal firing. *Nat. Neurosci.*, **7**, 1381–1386.
12. Chambers,J.J., Gouda,H., Young,D.M., Kuntz,I.D. and England,P.M. (2004) Photochemically knocking out glutamate receptors in vivo. *J. Am. Chem. Soc.*, **126**, 13886–13887.
13. Monroe,W.T., McQuain,M.M., Chang,M.S., Alexander,J.S. and Haselton,F.R. (1999) Targeting expression with light using caged DNA. *J. Biol. Chem.*, **274**, 20895–20900.
14. Minden,J., Namba,R., Mergliano,J. and Cambridge,S. (2000) Photoactivated gene expression for cell fate mapping and cell manipulation. *Sci. STKE*, **2000**, PL1.
15. Okamoto,H. (2007) Yin-Yang ways of controlling gene expression are now in our hands. *ACS Chem. Biol.*, **2**, 646–648.

16. Su,M., Yang,F., Lv,C., Yu,L., Gu,X., Wang,J., Li,Z. and Tang,X. (2010) Photoresponsive nucleic acids for gene regulation. *J. Chin. Pharm. Sci.*, **19**, 5–14.
17. Furuta,T. and Noguchi,K. (2004) Controlling cellular systems with Bhc-caged compounds. *Trends Anal. Chem.*, **23**, 511–519.
18. Heckel,A., Buff,M.C.R., Raddatz,M.-S.L., Mueller,J., Poetzsch,B. and Mayer,G. (2006) An anticoagulant with light-triggered antidote activity. *Angew. Chem. Int. Ed. Engl.*, **45**, 6748–6750.
19. Heckel,A. and Mayer,G. (2005) Light regulation of aptamer activity: An anti-thrombin aptamer with caged thymidine nucleobases. *J. Am. Chem. Soc.*, **127**, 822–823.
20. Hoebartner,C. and Silverman,S.K. (2005) Modulation of RNA tertiary folding by incorporation of caged nucleotides. *Angew Chem. Int. Ed. Engl.*, **44**, 7305–7309.
21. Kroeck,L. and Heckel,A. (2005) Photoinduced transcription by using temporarily mismatched caged oligonucleotides. *Angew. Chem. Int. Ed. Engl.*, **44**, 471–473.
22. Liu,Y. and Sen,D. (2004) Light-regulated catalysis by an RNA-cleaving deoxyribozyme. *J. Mol. Biol.*, **341**, 887–892.
23. Mayer,G. and Heckel,A. (2006) Biologically active molecules with a 'light switch'. *Angew. Chem. Int. Ed. Engl.*, **45**, 4900–4921.
24. Richard,J.L., Tang,X., Turetsky,A. and Dmochowski,I.J. (2008) RNA bandages for photoregulating in vitro protein translation. *Bioorg. Med. Chem. Lett.*, **18**, 6255–6258.
25. Tang,X. and Dmochowski,I.J. (2007) Regulating gene expression with light-activated oligonucleotides. *Mol. BioSyst.*, **3**, 100–110.
26. Casey,J.P., Blidner,R.A. and Monroe,W.T. (2009) Caged siRNAs for spatiotemporal control of gene silencin. *Mol. Pharmaceutics*, **6**, 669–685.
27. Mikat,V. and Heckel,A. (2007) Light -dependent RNA interference with nucleobase-caged siR. *RNA*, **13**, 2341–2347.
28. Shah,S., Jain,P.K., Kala,A., Karunakaran,D. and Friedman,S.H. (2009) Light-activated RNA interference using double-stranded siRNA precursors modified using a remarkable regiospecificity of diazo-based photolabile groups. *Nucleic Acids Res.*, **37**, 4508–4517.
29. Opalinska,J.B., Machalinski,B., Ratajczak,J., Ratajczak,M.Z. and Gewirtz,A.M. (2005) Multigene targeting with antisense oligodeoxynucleotides: an exploratory study using primary human leukemia cells. *Clin. Cancer Res.*, **11**, 4948–4954.
30. Rubenstein,M., Tsui,P. and Guinan,P. (2004) A review of antisense oligonucleotides in the treatment of human disease. *Drugs Future*, **29**, 893–909.
31. Ghosn,B., Haselton,F.R., Gee,K.R. and Monroe,W.T. (2005) Control of DNA hybridization with photocleavable adducts. *Photochem. Photobiol.*, **81**, 953–959.
32. Matsunaga,D., Asanuma,H. and Komiyama,M. (2004) Photoregulation of RNA digestion by RNase H with azobenzene-tethered DNA. *J. Am. Chem. Soc.*, **126**, 11452–11453.
33. Young,D.D., Lusic,H., Lively,M.O., Yoder,J.A. and Deiters,A. (2008) Gene Silencing in Mammalian Cells with Light-Activated Antisense Agents. *ChemBioChem.*, **9**, 2937–2940.
34. Corrie,J.E.T., Barth,A., Munasinghe,V.R.N., Trentham,D.R. and Hutter,M.C. (2003) Photolytic cleavage of 1-(2-nitrophenyl)ethyl ethers involves two parallel pathways and product release is rate-limited by decomposition of a common hemiacetal intermediate. *J. Am. Chem. Soc.*, **125**, 8546–8554.
35. Dussy,A., Meyer,C., Quennet,E., Bickle,T.A., Giese,B. and Marx,A. (2002) New light-sensitive nucleosides for caged DNA strand breaks. *ChemBioChem.*, **3**, 54–60.
36. Lenox,H.J., McCoy,C.P. and Sheppard,T.L. (2001) Site-specific generation of deoxyribonolactone lesions in DNA oligonucleotides. *Org. Lett.*, **3**, 2415–2418.
37. Ordoukhanian,P. and Taylor,J.-S. (1995) Design and synthesis of a versatile photocleavable DNA building block. Application to phototriggered hybridization. *J. Am. Chem. Soc.*, **117**, 9570–9571.
38. Tang,X. and Dmochowski,I.J. (2006) Controlling RNA digestion by RNase H with a light-activated DNA hairpin. *Angew. Chem. Int. Ed. Engl.*, **45**, 3523–3526.
39. Tang,X., Maegawa,S., Weinberg,E.S. and Dmochowski,I.J. (2007) Regulating gene expression in zebrafish embryos using light-activated, negatively charged peptide nucleic acids. *J. Am Chem. Soc.*, **129**, 11000–11001.
40. Tang,X., Swaminathan,J., Gewirtz,A.M. and Dmochowski,I.J. (2008) Regulating gene expression in human leukemia cells using light-activated oligodeoxynucleotides. *Nucleic Acids Res.*, **36**, 559–569.
41. Shah,S. and Friedman,S.H. (2007) Tolerance of RNA interference toward modifications of the 59 antisense phosphate of small interfering RNA. *Oligonucleotides*, **17**, 35–43.
42. Shestopalov,I.A., Sinha,S. and Chen,J.K. (2007) Light-controlled gene silencing in zebrafish embryos. *Nat. Chem. Biol.*, **3**, 650–651.
43. Ouyang,X., Shestopalov,I.A., Sinha,S., Zheng,G., Pitt,C.L.W., Li,W.-H., Olson,A.J. and Chen,J.K. (2009) Versatile Synthesis and Rational Design of Caged Morpholinos. *J. Am. Chem. Soc.*, **131**, 13255–13269.
44. Richards,J.L., Seward,G.K., Wang,Y.-H. and Dmochowski,I.J. (2010) Turning the 10-23 DNAzyme On and Off with Light. *ChemBioChem.*, **11**, 320–324.
45. Gangurde,R. and Modak,M.J. (2002) Participation of active-site carboxylates of Escherichia coli DNA polymerase I (klenow fragment) in the formation of a prepolymerase ternary complex. *Biochemistry*, 14552–14559.
46. Tang,X. and Dmochowski,I.J. (2005) Phototriggering of caged fluorescent oligodeoxynucleotides. *Org. Lett.*, **7**, 279–282.
47. Iwase,R., Kitani,A., Yamaoka,T. and Murakami,A. (2003) Synthesis of antisense oligonucleotides containing photocleavable protecting groups on the thymine bases and their photoinduced duplex formation. *Nucleic Acids Res. Supp.*, **3**, 61–62.